新型光学活性含氰基三联苯液晶聚噻吩合成与分子构象

谌　烈　　陈义旺*　　姚　凯　　周魏华　　李　璠　　聂华荣

(南昌大学化学系高分子研究所, 南昌　330031)

摘要：　合成了一种含有长柔性间隔基和氰基三联苯液晶基元的发光性聚噻吩衍生物{—[thiopheneyl—CH$_2$COO—(CH$_2$)$_6$—O—terphenyl—CN]$_n$—, PT(6)TPhCN}. 利用傅里叶变换红外(FT-IR)光谱、核磁共振(^{1}H NMR)、差示扫描量热(DSC)仪、偏光显微镜(POM)、紫外-可见(UV-Vis)吸收光谱和荧光(PL)光谱对单体和聚合物的结构及性质进行了表征. 单体都呈现出良好的液晶性能, 由于长间隔基的存在, 聚合物 PT(6)TPhCN 也呈现出良好SmA$_d$ 相. 氰基三联苯的存在还赋予了聚合物良好的光致发光性能, 同时, 长间隔基也有效地降低了分子间的相互作用, 进一步增强了聚合物的发光性能. 另外, 研究发现, 在未引入任何手性元素的情况下, 聚合物主链在圆二(CD)色谱还呈现出明显的 Cotton 效应, 这可能是由于大体积液晶基元的位阻效应和取向作用, 液晶基元环绕主链进行取向的同时诱导聚噻吩主链在长程范围内呈螺旋取向.

关键词：　光致发光；　液晶共轭聚合物；　三联苯；　聚噻吩；　螺旋构象
中图分类号：　O644；　O631.1+1

Synthesis and Helical Conformation of New Optically Active Liquid Crystalline Poly thiophene Containing Cyanoterphenyl Mesogen Pendant

CHEN Lie　　CHEN Yi-Wang*　　YAO Kai　　ZHOU Wei-Hua　　LI Fan　　NIE Hua-Rong
(*Institute of Polymers, Department of Chemistry, Nanchang University, Nanchang　330031, P. R. China*)

Abstract：　A novel liquid crystalline (LC) polythiophene bearing cyanoterphenyl mesogenic pendants with a long flexible spacer {—[thiophene—CH$_2$—COO—(CH$_2$)$_6$—O—terphenyl—CN]$_n$—, PT(6)TPhCN} was designed and synthesized. Structures of the monomer and the polymer were characterized by nuclear magnetic resonance (NMR) and Fourier transform infrared (FT-IR) spectroscopy while the liquid crystalline and other properties were evaluated with thermogravimetry, differential scanning calorimetry (DSC), polarized optical microscopy (POM), ultraviolet visibel (UV-Vis) spectroscopy and photoluminescence (PL). The monomer shows enantiotropic smectic phases during the heating and cooling processes. Because of the long flexible spacer, the polymer PT(6)TPhCN exhibits a colorful SmA$_d$ mesogenic phase texture. The cyanoterphenyl group results in the polymer having good photoluminescence. The spacer length also greatly influences the UV absorption and photoluminescence behavior of the polymers. A longer spacer may better segregate the backbone, which effectively enhances the stronger photoluminescence emission. More interestingly, without introducing any chiral groups, the polymer exhibits an obvious Cotton effect on the circular dichroism (CD) spectra, which results from the predominant screw sense of the backbone. This is probably due to the heavy bulky mesogenic pendant rotating around the polythiophene backbone and producing a backbone with a helical conformation in the long wavelength region.

Key Words：　Photoluminescence；　Liquid crystalline conjugated polymer；　Cyanoterphenyl；　Polythiophene；　Helical conformation

Combining liquid crystallinity (LC) and luminescence into the polymer, liquid crystalline conjugated polymers (LCCP) are currently drawing interest from the viewpoint of multifunctional electrical and optical materials[1–4]. Attracted by the application perspective, recently, a variety of LCCP based on different conjugated main chain have been prepared, which can be endowed with such functional properties as mesomorphism, luminescence, photoconductivity, gas permeability, chain helicity[5–20]. Especially, a polymer with the two electrooptical features (both liquid crystalline and light emitting) is of practical value, which may offer very high carrier mobility and emit polarized light and may find unique applications and stimulate technological innovations in the development of novel electronic and photonic devices[21]. Tang *et al.*[22–23] synthesized a series of polyacetylenes bearing light emitting chromophore with different functional bridges and spacer length, they found that the light emitting chromo-phore endows the polymer with high luminescence and the spacer length plays an important role in the packing arrangement of the mesogens.

Polythiophene and its processable derivatives occupy an important position in the study of conjugated polymers. The polythiophenes have many attractive characteristics such as good electrical properties and stability, for application in polymer electroluminescence devices[24]. Polythiophene derivatives with LC side chains are one of the most intriguing types of polymer because their useful electrical and optical properties are expected to be controllable *via* the molecular orientation of LC side chain. Allso, it is expected that the orientation of the LC side chain may enhance the main-chain coplanarity due to the spontaneous orientation of the LC group of the side chains. The main-chain orientation can be further improved and therefore results in improved electrical properties. A variety of polythiophenes containing liquid crystalline mesogens and light-emitting chromophores have been prepared[25–34].

The terphenyl core has a calamitic structure that is compatible with mesomorphic ordering and is well known to give liquid crystals that have high birefringence[35–36]. In our pervious studies, we have synthesized a type of polyacetylene and poly(*p*-phenylene) containing cyanoterphenyl mesogen and found that the cyanoterphenyl mesogen pendants endow the polymer with good mesomorphism and high luminescence, besides, the energy could be transferred from mesogen to main chain to favor the fluorescence efficiency [37–40]. Since polythiophenes have so many att ractive characteristics for application, we also synthesized polythiophene PT(0)TPhCN containing cyanoterphenyl mesogen as pendant —[thiophene—CH₂—COO—terphenyl—CN]ₙ— (Shown in Scheme 1)[41]. However, the short spacer between the mesogenic pendant and the polythiophene backbone results in the loss of liquid crystallinity. Thus, in this work, we designed a novel polythiophene bearing cyanoterphenyl mesogen with long flexible spacer length —[thiophene—CH₂—COO—(CH₂)₆—O— terphenyl—CN]ₙ—, and hope that the long relatively flexible spacer could allow the mesogens to undergo thermal transitions

in an independent fashion and to maintain its mesomorphism. This article presents the influence of the structure of polythiophene on its properties. A comparison has also been made between the polymers with short spacer and the one with long spacer. Besides, due to the stereoeffect, the bulkly mesogens the backbone probably orientates around the polythiophene backbone and induces the backbone with helical conformation in the long region. Therefore, the secondary structures of polymers have also been investigated.

1 Experimental

1.1 Materials

Trimethyl borate (99%), *n*-butyllithium (2.87 mol·L⁻¹ in hexane), thiophene-3-acetic acid (98%), 6-bromo-1-hexanol (98%), trimethyl borate, 4-(4-bromophenyl)phenol (97%), 4-bromobenzonitrile (95%), 1,3-dicyclohexylcarbodiimide (DCC)(95%), and 4-(dimethylamino)pyridine (DMAP) (99%) and tetrakis (triphenylphosphine) palladium were purchased from Alfa Aesar and used as received without any further purification. Tetrahy-drofuran (THF) was dried over sodium. Other chemicals were obtained from Shanghai Reagent Co., Ltd., and used as received.

1.2 Techniques

The nuclear magnetic resonance (NMR) spectra were collected on a Bruker ARX 400 NMR spectrometer with deuterated chloroform or THF or (DMSO) as the solvent and with tetramethylsilane (δ=0) as the internal standard. The infrared (IR) spectra were recorded on a Shimadzu IRPrestige-21 Fourier transform infrared (FTIR) spectrophotometer by drop-casting sample solution on KBr substrates. The ultraviolet-visible (UV-Vis) spectra of the samples were recorded on a Hitachi UV-2300 spectrophotometer. Fluorescence measurement for photoluminescence (PL) of the polymers was carried out on a Shimadzu RF-5301 PC spectrofluorophotometer with a xenon lamp as the light source. The gel permeation chromatography (GPC), so-called size-exclusion chromatography (SEC) analysis, was conducted with a Breeze Waters system equipped with a Rheodyne injector, a 1515 Isocratic pump and a Waters 2414 differential re-fractometer using polystyrenes as the standard and THF as the eluent at a flow rate of 1.0 mL·min⁻¹ and 40 ℃ through a Styragel column set, Styragel HT3 and HT4 (19 mm×300 mm, 10²+10³ nm) to separate molecular weight (M_w) ranging from 10² to 10⁶. Thermogravimetric analysis (TGA) was perfor-med on a Perkin Elmer TGA 7 for thermogravimetry at a heating rate of 20 ℃·min⁻¹ under nitrogen with a sample mass of 8−10 mg. Differential scanning calorimetry (DSC) was used to determine phase-transition temperatures on a Perkin-Elmer DSC 7 differential scanning calorimeter with a constant heating/cooling rate of 10 ℃·min⁻¹. Texture observations by polarizing optical microscopy (POM) were made with a Nikon E600POL polarizing optical microscope equipped with an Instec HS 400 heating and cooling stage. The X-ray diffraction (XRD) study of the sam-ples was carried out on a Bruker D8 Focus X-ray diffractometer operating at 30 kV and 20 mA with a copper target (λ=0.154 nm) and at a scanning rate of

1 (°)·min⁻¹. Circular dichroism (CD) spectrum was recorded on a JASCO J-810 spectropolarimeter.
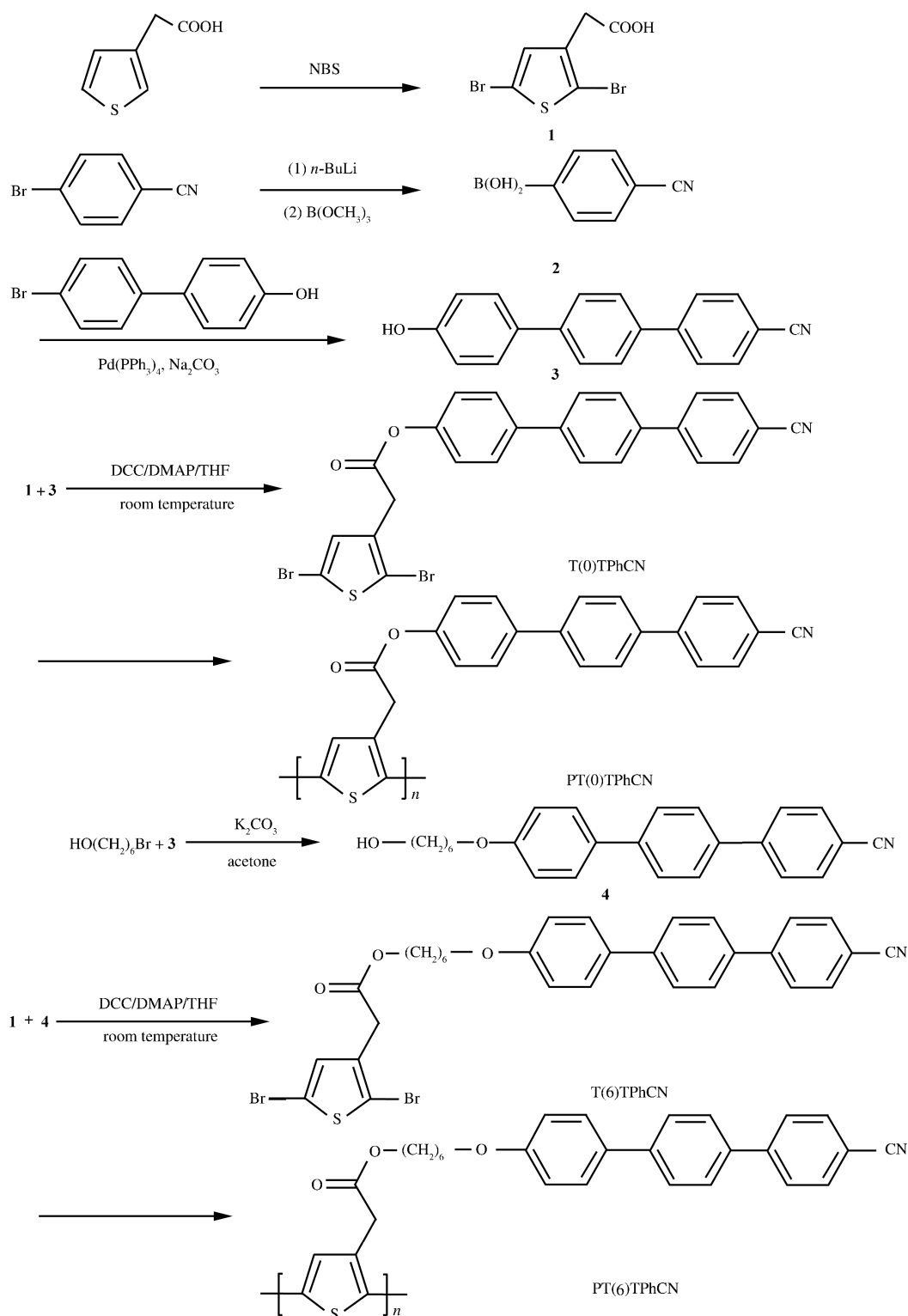
1.3   Synthesis of the monomer

The synthesis and structures of the monomer are outlined in Scheme 1. All the reactions and manipulations were carried out

under nitrogen atmosphere.

1.3.1   2,5-Dibromothiophene-3-acetic acid (**1**)

Thiophene-3-acetic acid (10 g, 70.3 mmol) was very slowly added to a solution of *N*-bromosuccinimide, NBS (30.2 g, 172 mmol), in 50 mL of DMF by a dropping funnel. After the addi-

Scheme 1   Illustration of procedures for synthesis of the monomers and their polymerization

tion, 10 mL of DMF was further added to the reaction mixture and refluxed at 50 ℃ for 20 h under argon atmosphere. The reaction vessel was wrapped by aluminum foil to shield the reaction from light. When the reaction finished, the reaction mixture was allowed to warm to room temperature. The solution was poured into a large amount of saturated sodium sulfate cooled by ice water. The yellow precipitate was filtered off and recrystallized from an ethanol/water mixture to yield product as white needlelike crystal. Yield: 63.0%. IR (cm^{-1}): 3101, 2918, 1707, 1415, 1327, 1232, 1016, 829, 735, 632, 469. ^{1}H NMR (CDCl$_3$, from TMS): δ 3.63 (s, 2H, CH$_2$), 6.95 (s, 1ArH, BrC-CHC).

1.3.2 4-Cyanobenzeneboronic Acid (2)

A solution of *n*-butyllithium (30 mL, 2.87 mol·L^{-1} in hexane, 0.086 mol) was added dropwise to a stirred, cooled (−110 ℃) solution of 4-bromobenzonitrile (15 g, 0.082 mol) in dry THF (180 mL) under dry nitrogen. The solution was stirred at −100 ℃ for 1 h and a solution of trimethyl borate 20.8 mL in dry THF (60 mL) was added at −100 ℃. The solution was allowed to warm to room temperature overnight. 10 percent hydrochloric acid was added and the solution was stirred for 1 h at room temperature. The product was extracted into ether and the organic layer was washed with water and dried with MgSO$_4$. The solvent was removed *in vacuo* and the crude product dis-solved in THF and precipitated with *n*-hexane to give a yellow solid with yield of 70%.

1.3.3 4-Hydroxy-4 -cyanoterphenyl (3)

Under dry nitrogen atmosphere a solution of 2.00 g of 4-cyanobenzeneboronic acid (13.6 mmol) in 10 mL of ethanol was added to a solution of 2.75 g of 4-(4-bromophenyl)phenol (97%, 11.02 mmol) and 0.42 g of tetrakis(triphenylphosphine)palladium(0) (99%, 0.36 mmol) in 20 mL of benzene and 20 mL of aqueous Na$_2$CO$_3$ (2 mol·L^{-1}). The reaction was conducted under reflux overnight. The reaction mixture was then shaken with ethyl acetate and the insoluble parts were filtered off. The organic layer was dried with anhydrous MgSO$_4$, and the solvent was removed by evaporation *in vacuo*. The crude product was recrystallized from acetone to provide a yellow powder, 65% yield. IR (KBr, cm^{-1}): 2215 (C≡N), 3351 (—OH). ^{1}H NMR (CDCl$_3$): δ 7.73−7.65 (m, 8H, aromatic), 7.53 (d, 2H, aromatic), 6.93 (d, aromatic, 2H ortho to hydroxyl), 4.91 (s, 1H, —OH).

1.3.4 4-(6-Hydroxyhexyloxy)-4 -cyanoterphenyl (4)

Mixing 20 mmol of (3), 24 mmol of 6-bromo-1-hexanol, 40 mmol of K$_2$CO$_3$ and 4.01 mmol of KI in 200 mL of DMF, the reaction mixture was refluxed at 80 ℃ for 24 h. And then cooled and the solvent was removed by evaporation *in vacuo*. The residue was recrystallized from absolute ethanol to give a light yellow solid in 73% yield. IR (KBr, cm^{-1}): 3416, 3033, 2935, 2852, 2228, 1600, 1491, 1258, 1047, 812. ^{1}H NMR (THF-d): δ 7.64−7.77 (m, 8H, aromatic), 7.58−7.62 (d, 2H, aromatic), 6.87−6.89 (d, aromatic, 2H), 4.55 (t, 1H, —OH), 3.89−3.92 (t, 2H, —CH$_2$OAr—), 3.36−3.39 (t, 2H, —CH$_2$OOC), 1.33−1.72 (m, 8H, —(CH$_2$)$_4$).

1.3.5 2,5-Dibromo-3-{[[6-[4-(4 -cyano)terphenyloxy]hexyloxy]carbonyl] methyl}-thiophene (T(6)TPhCN)

2,5-Dibromothiophene-3-acetic acid (3.43 g, 12 mmol) was added to a mixture of (4) (3.71 g, 10 mmol), (dimethylamino) pyridine, DMAP 1.47 g (12 mmol), and dicyclohexylcarbodiimide, DCC (2.46 g, 12 mmol), in 200 mL of absolute THF and further stirred for 24 h at room temperature under argon atmosphere. Then the solution was filtered to remove the urea crystals, and the solvent was removed by evaporation. The crude product was purified by column chromatography (*n*-hexane/CHCl$_3$ volume ratior of 1/4) to afford T(6)TPhCN as white powder. Yield =75%. IR (KBr, cm^{-1}): 2948, 2862, 2228, 1731, 1592, 1483, 1007, 810, 641. ^{1}H NMR (CDCl$_3$): δ 7.74−7.63 (m, aromatic, 8H), 7.58, 7.56 (d, aromatic, 2H), 7.05, 7.00 (d, aromatic, 2H ortho to —O—), 6.98 (s, aromatic, 1H, BrCCHC), 4.15−4.12 (t, 2H, —CH$_2$—O—Ar), 4.03−4.00 (t, 2H, —CH$_2$—OOC—), 3.57 (s, 2H, —CH$_2$—COO—), 1.84−1.42 (m, 8H, —CH$_2$(**CH$_2$**)$_4$CH$_2$—).

1.4 Polymerization

The polymerization reaction and manipulations were carried out under nitrogen using Schlenk techniques in a vacuum line system or in an inert-atmosphere glovebox (vacuum atmospheres), except for the purification of the polymer, which was done in an open atmosphere.

A 50 mL three-neck round bottom flask equipped with condenser, rubber septum, nitrogen inlet-outlet and magnetic stirrer was charged under nitrogen with 0.655 g (1.0 mmol) T(6)TPhCN, 0.08 g (0.0304 mmol) PPh$_3$, 2.024 g (30.96 mmol) Zn, 0.0076 g (0.05 mmol) bpy, 0.0064 g (0.05 mmol) NiCl$_2$ and 5 mL of dry dimethyl acetamide (DMAC). The reaction was performed at 85 ℃ under nitrogen. The mixture was stirred for 24 h. Then, the polymer was precipitated in excess methanol/HCl mixture, filtered and dried. The polymer was then redissolved in THF and precipitated in methanol. A red-brown solid was obtained.

PT(6)TPhCN, red-brown solid: IR (KBr, cm^{-1}): 2932, 2856, 2215, 1731, 1599, 1487, 1245, 1103, 803. ^{1}H NMR (DMSO-d$_6$): δ 7.74−7.48(m, 10H, aromatic), 7.02−6.96(m, aromatic, 2H ortho to —O— and 1 H, BrCCHC), 4.05 (m, 2H, —CH$_2$—O—Ar), 3.96 (m, 2H, —CH$_2$—OOC—), 3.50 (s, 2H, —CH$_2$—COO—), 1.69−1.37 (m, 8H, —CH$_2$(**CH$_2$**)$_4$CH$_2$—). Weight-average molecular weight (M_w) is 20100; Number-average molecular weight (M_n) is 11500; and M_w/M_n=1.75.

2 Results and discussion

2.1 Synthesis of monomer and polymer

3-Position substituted thiophene is prepared by Suzuki reaction, etherification and esterification, in sequence. The synthetic route of the monomer is shown in Scheme 1. The terphenyl mesogen is obtained *via* Suzuki reaction. The monomer is synthesized through esterification reaction route in the presence of 1,3-dicyclohexylcarbodimine (DCC) and 4-(dimethylamino)pyridine (DMAP). The reaction goes smoothly, and the product is isolated in high yield near 70% after purifications by silica gel chromatography followed by recrystallization. All the intermediates and final products are thoroughly purified and fully characterized, and satisfactory analysis data are obtained (detailed spectroscopic data for the key intermediates and for all the com-

pounds being given in the Experimental Section).

The polymerization of 2,5-dibrominated thiophene monomer was carried out *via* dehalogenative polycondensation, giving poly-(3-position substituted thiophene) derivative, PT(6)TPhCN. The polymer synthesized was fusible and soluble in common organic solvents including tetrahydrofuran (THF), DMAC, DMSO and DMF, etc. Number-average (M_n) and weight-average (M_w) molecular weights of the polymer are summarized in the Experimental Section. The chemical structure of the polymer is confirmed by FT-IR and ^{1}H NMR.

2.2   Structural characterization

Substituted thiophene and its corresponding polymer are characterized by spectroscopic methods and all the products give satisfactory data corresponding to their expected molecular structures. A typical example of the IR spectra of PT(6)TPhCN is shown in Fig.1. The spectrum of its monomer T(6)TPhCN is also shown in the same figure for comparison. The C═O and C≡N absorption bands of the monomer and polymer are observed at about 1731 and 2228 cm^{-1}, respectively. The strong C—H stretch absorption is located at 3000 cm^{-1}. When the monomer is polymerized by dehalogenative polycondensation, the C—Br bending vibration absorption band (about 500 cm^{-1}) disappears in the spectra of its polymer, which means that the monomer has been polymerized successfully. Fig.2 shows the ^{1}H NMR spectrum of the isolated polymer in comparison with that of monomer, which sufficiently supports the structures of the products by the assignments of the signals as described in the experimental section. Monomer T(6)TPhCN and its polymer have the similar resonance peaks in their ^{1}H NMR spectra. The aromatic H resonance peaks appear in the low magnetic region (δ 7.0−8.0), whereas the aliphatic H resonance peaks in the high magnetic region (δ 1.8−1.3), except the peaks of the near-neighboring aliphatic H to the —O— or —CO— shifted to the middle region (δ 4.0−3.5). All the resonance peaks of the polymer show much broader than that of its monomer, which further confirms the perfect conversion from monomer to polymer. Except the peaks of solvent and water remained in the spectra, no unexpected signals are observed in the spectra of the monomer and
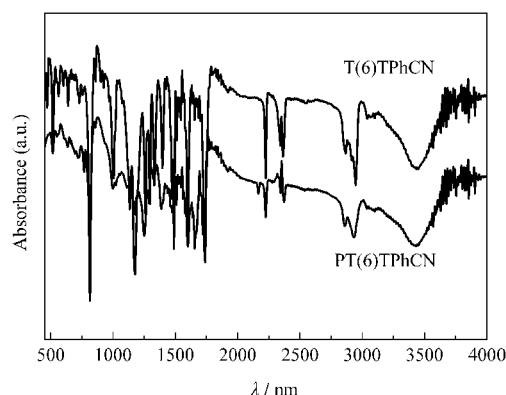

Fig.1   FT-IR spectra of the monomer T(6)TPhCN and polymer PT(6)TPhCN

polymer, and all the resonance peaks can be assigned to appropriate protons as marked in Fig.2.

2.3   Thermal stability

Since the formation of mesophases of thermotropic liquid crystals are realized by the application of heat, the thermal stability of the polymer is thus of primary concern. The polymer PT(6)TPhCN exhibited excellent thermal stability. As shown in Fig.3, the polymer PT(6)TPhCN decomposed at a temperature as high as ca 350 ℃ in the thermogravimetric analysis. The thermal stability originates from the "jacket" effect of the terphenyl mesogenic appendages well wrapping the conjugated backbones and protecting the conjugated backbone from the perturbations by heat attack[22].

2.4   Mesomorphic properties

The thermal transition behaviors of the monomer and polymer are examined by differential scanning calorimetry (DSC) and polarized optical microscopy (POM). The polarized optical microscopy textures of the monomer and polymer are displaye d in Fig.4. The monomer T(6)TPhCN exhibits optical anisotropy when observed by POM, suggesting that the terphenyl mesogens endow the compound with thermotropic liquid-crystalline behaior. When the monomer is cooled from its isotropic state, many batonnets emerge from the dark background and grow to bigger domains, leading to the formation of the focal conic texture
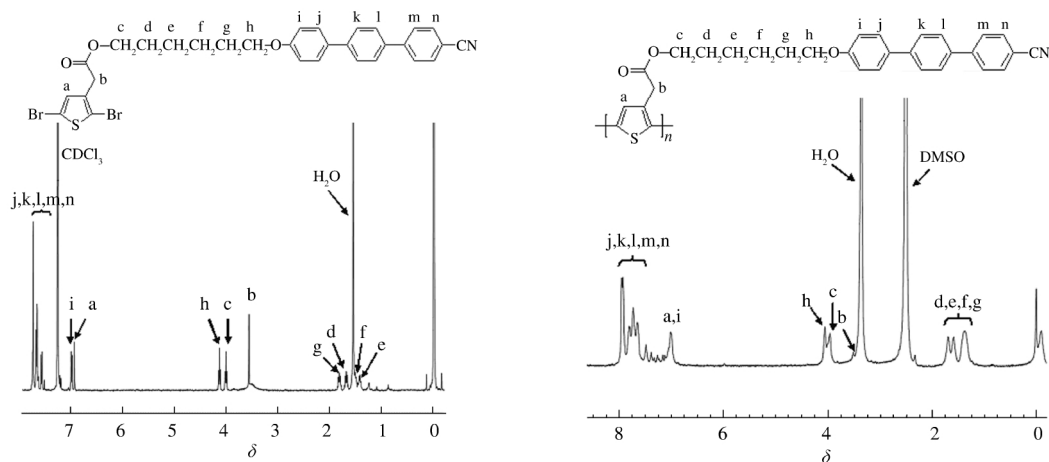

Fig.2 ^{1}H NMR spectra of the monomer and polymer

characteristic of the smectic phase. The birefringent texture also can be observed by reheating the solid states. In our previous study, the polymer PT(0)TPhCN with short aster spacer could not exhibit any optical anisotropy when heated or cooled, indicating that the polymer is completely nonmesomorphic. Because the mesogenic pendant is closely "coupled" with the rigid back-bone, it destroys the packing arrangements of the mesogens and demolishes the stability of the mesophases[37,42]. Cheerfully, different from PT(0)TPhCN, with the favoring of flexible long spacer, the PT(6)TPhCN shows bright colorful texture when heating and cooling, and with the aid of XRD analysis the texture is identified with SmA_d, indicating that the PT(6)TPhCN is indeed enantiotropic liquid crystalline. This suggests that the polythiophene backbones and the terphenyl mesogens are well "decoupled" and the flexibility of the long spacer allows the mesogen to move together to pack in a regular fashion.

To learn more about the thermal transitions of the monomer and polymer, we measured their thermograms under nitrogen on a differential scanning calorimeter (shown in Fig.5). The DSC thermogram of T(6)TPhCN shows two transition peaks at 96.5 and 104.8 ℃ in the second heating cycle, associated with k-SmA_d and SmA_d-i transtions, respectively. Their corresponding i-SmA_d and SmA_d-k transtions do not exhibited in the first cool-
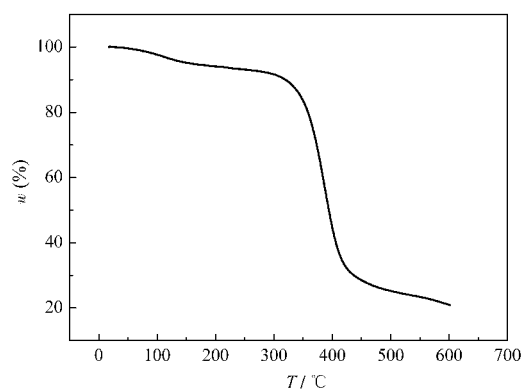

Fig.3   TGA thermogram of polymer under nitrogen at a heating rate of 20 ℃·min^{-1}

ing scan, probably due to the fast cooling rate, but, the focal conic texture is obvious under POM, indicating an enantiotropic smecticity. Different from the DSC curve of PT(0)TPhCN which does not show any peaks associated with the liquid phase transition, polymer PT(6)TPhCN with longer flexible spacer length appears two transtions at 209.0 and 289.6 ℃ in the seconding curve, indicating that the longer spacer offers more freedom for the polymer segments and the mesogenic pendants to act separately. But compare to T(6)TPhCN, the temperatures of the two
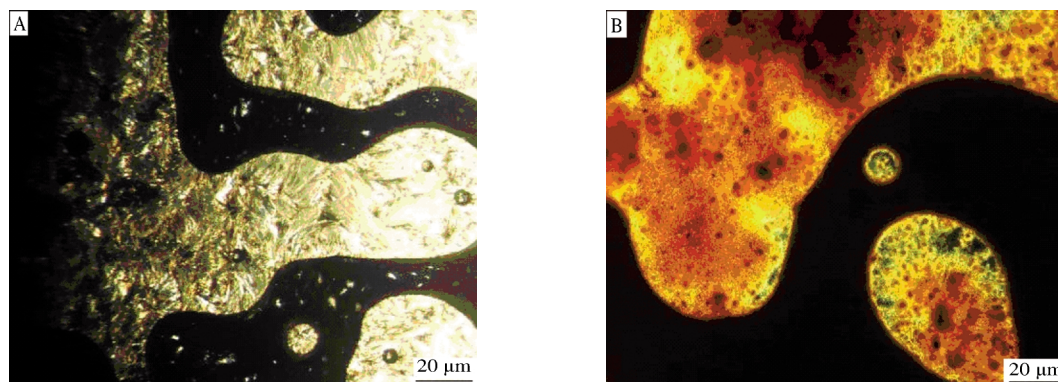

Fig.4   Smectic phase textures observed by POM at 102 ℃ for T(6)TPhCN (A) and at 232 ℃ for PT(6)TPhCN (B) under cooling from melt state
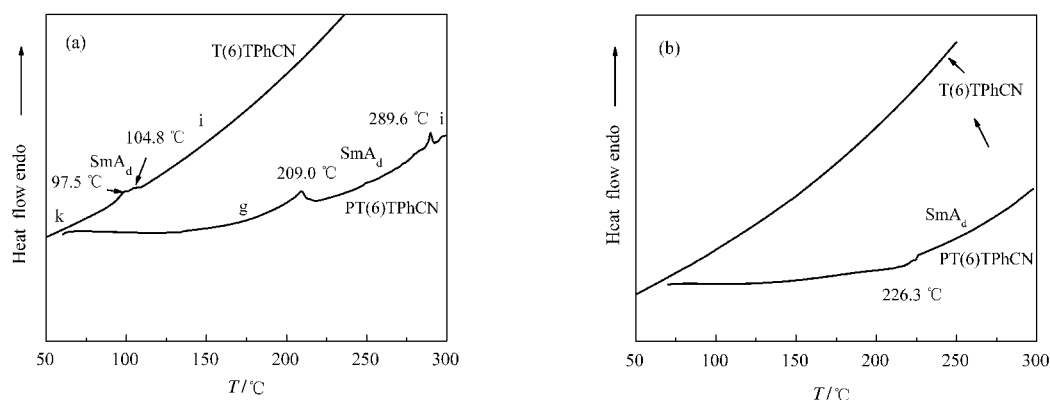
cooling rate: 1 ℃·min^{-1}

Fig.5   DSC thermograms of the monomer and polymer recorded under nitrogen during (a) the second heating scans and (b) the first cooling

scan rate: 10 ℃·min^{-1}

trans- tions of PT(6)TPhCN are much higher than that of its cor–respon-ding monomer. Apparently, the mesogenic pendants are not com-pletely "decoupled" from the polymer main chains, and the "poly- mer effect" is functioning. The macromolecular chains string the mesogenic pendants together in a comblike fashion, making the mesogens easy to order but difficult to ran–domize, as argued by other scientists[13].

XRD analysis can provide useful information concerning molecular arrangement, mode of packing, and type of order in a mesophase of a polymeric liquid crystal. WAXD patterns of the polymer and monomer were obtained at room temperature after the samples had been quenched from liquid-crystalline states with liquid nitrogen. The diffractogram of a powder sample can be generally divided into the low-angle Bragg reflections corresponding to the layer spacing of molecular orientational order and the high-angle peaks associated with the liquidlike interme-sogenic organization within the layers. The appearance of a broad or sharp peak serves as a qualitative indication of the degree of order[43]. T(6)TPhCN shows an typical smectic phase XRD patter consisting of one low-angle peak ($2\theta=2.28°$) and one high-angle peak ($2\theta=21.01°$) (Fig.6). The d-spacing derived from the low-angle peak is 3.850 nm, which is excess of the calculated molecular length (l) of T(6)TPhCN in its most extended confor-mation ($l=2.801$ nm), but less than the double of molecular length, thus, the T(6)TPhCN shows the nature of SmA_d phase with bi-layer arrangement, where the mesogens are interdigitated in an antiparallel fashion. The diffractogram of PT(6)TPhCN quenched from 269 ℃ exhibits a broad peak at $2\theta=19.99°$, from which a d-spacing of 0.448 nm is derived from Bragg's law, occurring in the lateral packing arrangement of the mesogenic pendants. The layer spacing (d) derived from the Bragg reflection at $2\theta=2.04°$
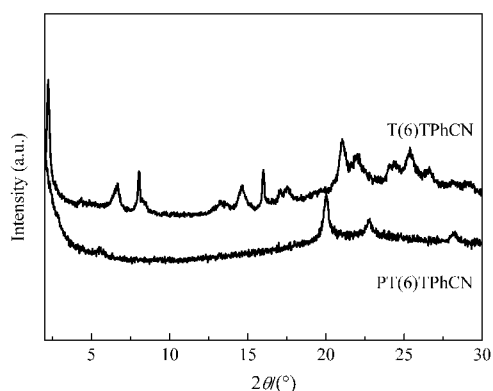

Fig.6   XRD patterns of the monomer and polymer quenched from their liquid crystalline states

($d=4.271$ nm) is longer than the molecular length ($l=2.756$ nm) of one repeat unit of PT(6)TPhCN at its most extended conforma-tion. Because the d/l ratio is ca 1.5, the bilayer structure is thus an $SmAd$ type as schematically shown in Fig.7, in which the mesogens arrange in an antiparallel overlapping interdigitated manner. In the mid-angle region, the diffractogram of the poly-mer PT(6)TPhCN shows a weak reflection at $2\theta=5.52°$, from which a d-spacing of 1.597 nm. The calculated length for the in-terdigitated (cyanoterphenylyl)oxy groups in the proposed bilay-er structure of PT(6)TPhCN is 1.516 nm. The reflection peak at $2\theta=5.52°$ thus may be related to the regions, in which the rigids (cyanoterphenylyl)oxy are interdigitated and well packed. The results are as well as identified with the POM and DSC.

2.5   Electronic absorption and photoluminescence

The electronic absorption spectra and photoluminescence of CH_2Cl_2 solutions of the polymer PT(6)TPhCN and monomer T(6)TPhCN are given in Fig.8 and Fig.9, respectively. In order to
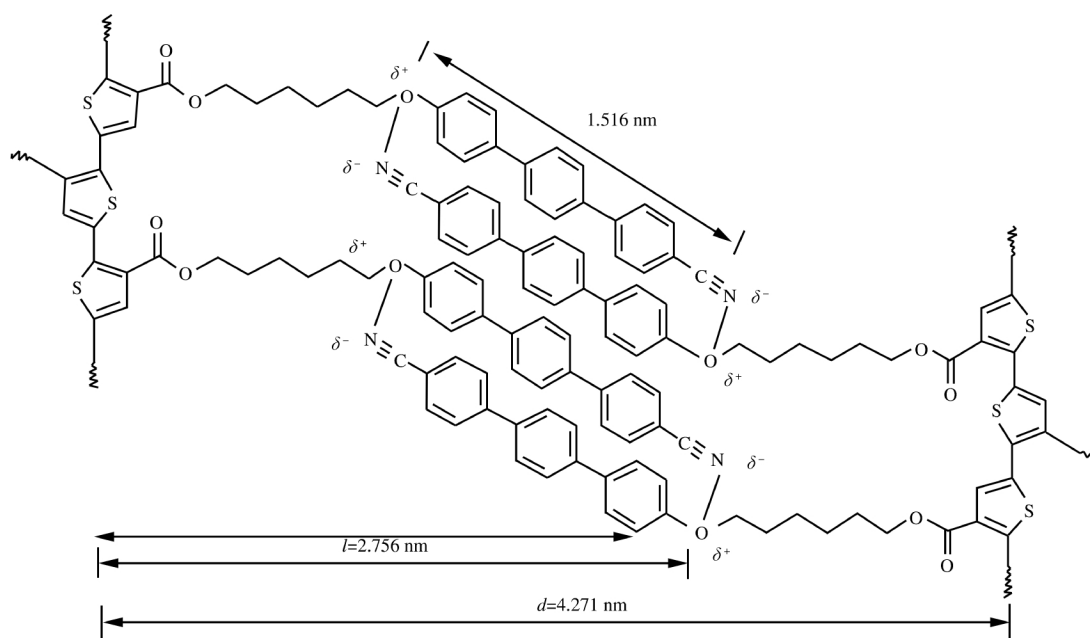

Fig.7   Proposed bilayer packing arrangement of PT(6)TPhCN within the SmA_d layer with the smectogens interdigitating in antiparallel fashion

make a comparison between the two polymers, the spectra of the polymer PT(0)TPhCN and its monomer T(0)TPhCN have also been given. Due to the cyanoterphenyl chromophore, the monomers and polymers have the similar absorption wavelengths at about 300 nm, which are assignable to the $\pi-\pi^*$ bands of the cyanoterphenyl mesogenic pendants. The absorptions of the polymers are stronger than that of its corresponding monomers and the absorption in the long-wavelength visible spectral region is thus obviously from the polythiophene backbone. The low absorptivity of the polymer PT(0)TPhCN main chain may have been due to the reduction of the effective conjugation lengths along the polymer backbone caused by steric effect. The intensity of PT(6)TPhCN in the long-wavelength region is much stronger than that of PT(0)TPhCN, Which is in agreement with our previous observations[37,39] that the longer spacer reduces steric crowding and allows backbone to be more coplanar than the short spacer, thus resulting in the observed hyperchromic effect.

Since polythiophenes derivatives bear chromophoric pendant groups, it is of interest to check the effects of the structural variables on luminescence behaviors of polymers. Upon photoexcitation at 300 nm, the two strong light emitting bands at 380 and 425 nm observed for the solution of PT(0)TPhCN are assigned to the emitting center of the cyanoterphenyl mesogenic core and that of the conjugated polythiophene main chain (shown in Fig.9), which suggests that the emitting center is both the cyanoterphenyl mesogenic pendant and the backbone. The light emitting bands of the mesogens and backbones also emerge in the PL spectrum of the PT (6)TPhCN. As can be seen from the spectra shown in Fig.8 and Fig.9, the thiophene backbone absorbs in a spectral region where its cyanoterphenyl pendant emits. Therefore, the excitation pumps its cyanoterphenyl pendant to the excited state, the UV light emitted from the pendant is reabsorbed by the backbone, suggesting that energy transfer from the cyanoterphenyl pendants to the backbone favors the stronger light-emitting of backbone. The absorption of the PT(6)TPhCN with the longer spacer inserted between the backbone and mesogenic pendant is about 30 nm red-shifted than that of PT(0)TPhCN, even extending to near 600 nm. The result is in agreement with the Tang′s observation[17] that the longer flexible spacers have bet-
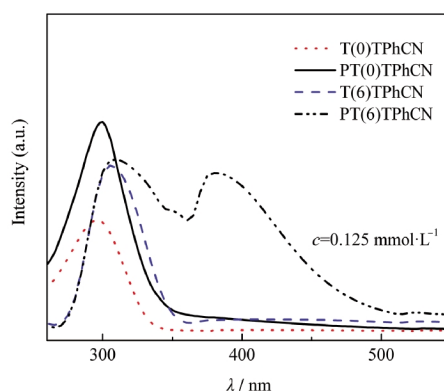

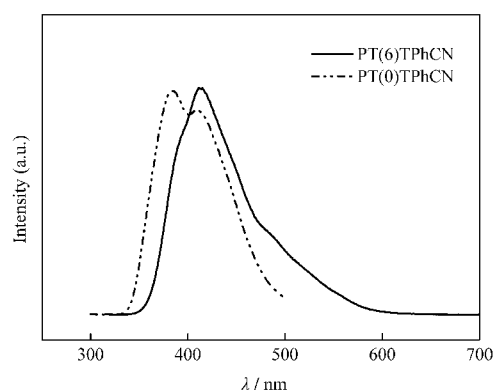**Fig.9　Photoluminescence spectra of polymers in CH₂Cl₂ solutions**

$c=0.125$ mmol·L⁻¹; excitation wavelength: 300 nm

ter keep the conjugated backbone apart and further enhance stronger photolumincescence.

2.6　Secondary structure of the polymers

Synthetic helical polymers with π-conjugation along the main chains is under hot pursuits in recent years due to the challenge they offer in polymer chemistry as well as their wide practical and potential applications, such as optical polarizing films, chiral stationary phases, asymmetric electrodes, nisotropic molecular wires, fluorescent chemosensors[44]. Generally, helical conjugated polymers are obtained by the introduction of chiral substituents, polymerization using a chiral catalystic system, or preparation in a chiral liquid crystalline solvent, a new method reported by Goto[45].

As we mentioned above, the heavy bulkly mesogenic pendants of PT(0)TPhCN are closely "coupled" with the rigid backbone and even those of PT(6)TPhCN with longer spacers are not completely "decoupled", that is, to avoid steric crowding, the heavy bulkly mesogens probably rotate around the main chain to induce the main chain with helical tendency. It is interest of check how the heavy bulk mesogen exert its influence on the backbone, thus, the CD spectrum is measured to prove our assumption. The CD spectra of PT(0)TPhCN and PT(6)TPhCN measured in THF is shown in Fig.10. Although there have no any chiral groups/center in the structures of the polymers, PT(0)TPhCN
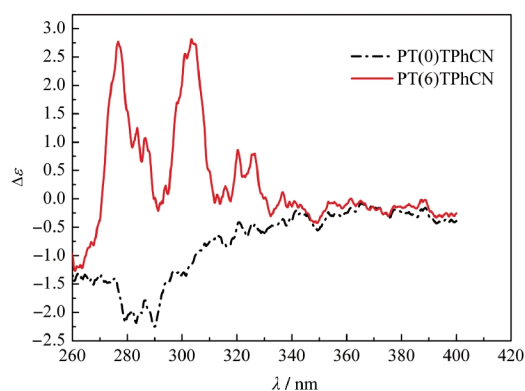

Fig.8　UV-Vis spectra of the monomers and polymers in CH₂Cl₂ solutions

Fig.10　CD spectra of the polymers measured in THF

$c=0.25$ mmol·L⁻¹

shows several negative CD band at 284, 293, and 313 nm, while PT(6)TPhCN exhibits several positive Cotton effect at 278, 289, 300, and 317 nm, which unambiguously confirms that these polymers adopt a helical conformation with a preferred screw sense. Due to no chiral groups existing in the polymers, thus the helical conformation must originate from the backbone. Therefore, introducing the heavy bulky as the pendant linked to the backbone will be a novel charming method to obtain helical polymers.

3　Conclusions

In this work, we designed and synthesized a novel polythiophene, and introduced the chromophoric cyanoterphenyl mesogenic pendant onto the polythiophene main chain with long flexible spacer length. The effects of the structural variations on the chemical and physical properties of the monomer and polymer were investigated. Owning to the protective jacket effect contributed by cyanoterphenyl mesogenic pendant, the polymer is thermally very stable. The long flexible spacer length is in favor of the mesomorphic properties, the UV absorption and photoluminescence of the polymers.

A significant and interesting finding also can be observed in this type of polymers: in order to reduce the repellent from steric crowding, the cyanoterphenyl mesogen pendant orientating around the skeleton can force the main chain to be helical conformation in the long region. Thus, without using any chiral element, we can obtain helical polymers easily only by introducing the heavy bulky as the pendant linked to the backbone. Understanding the relationship between the structure and properties may widen and deepen our knowledge on how to design the molecular structure and may provide us with a newly way to obtain polymers with the helical conformation.

References

1　Kuroda, H.; Goto, H.; Akagi, K.; Kawaguchi, A. *Macromolecules*, **2002, 35**: 1307

2　Burroughes, J. H.; Bradley, D. D. C.; Brown, A. R.; Marks, R. N.; Mackay, K.; Friend, R. H.; Burns, P. L.; Holmes, A. B. *Nature*, **1990, 347**: 539

3　Bowman, D.; Mattes, B. R. *Synth. Met.*, **2005, 154**: 29

4　Lee, K.; Cho, S.; Park, S. H.; Heeger, A. J.; Lee, C. W.; Lee, S. H. *Nature*, **2006, 441**: 65

5　Yuan, W. Z.; Sun, J. Z.; Dong, Y.; Haeussler, M.; Yang, F.; Xu, H. P.; Qin A.; Lam, J. W. Y.; Zheng Q.; Tang, B. Z. *Macromolecules*, **2006, 39**: 8011

6　Akagi, K.; Guo, S.; Mori, T.; Goh, M.; Piao, G.; Kyotani, M. *J. Am. Chem. Soc.*, **2005, 127**: 14647

7　Xing, C.; Lam, J. W. Y.; Zhao, K.; Tang, B. Z. *J. Polym. Sci. A-Polym. Chem.*, **2008, 46**: 2960

8　Zhou, J. L.; Chen, X. F.; Fan, X. H.; Chai, C. P.; Lu, C. X.; Zhao, X. D.; Pan, Q. W.; Tang, H. Y.; Gao, L. C.; Zhou, Q. F. *J. Polym. Sci. A-Polym. Chem.*, **2006, 44**: 4532

9　Sanda, F.; Araki, H.; Masuda, T. *Macromolecules*, **2004, 37**: 8510

10　Lai, L. M.; Lam, J. W. Y.; Qin, A.; Dong, Y.; Tang, B. Z. *J. Phys. Chem. B*, **2006, 110**: 11128

11　Li, B. S.; Kang, S. Z.; Cheuk, K. K. L.; Wan, L.; Ling, L.; Bai, C.; Tang, B. Z. *Langmuir*, **2004, 20**: 7598

12　Yuan, W. Z.; Mao, Y.; Zhao, H.; Sun, J. Z.; Xu, H. P.; Jin, J. K.; Zheng, Q.; Tang, B. Z. *Macromolecules*, **2008, 41**: 701

13　Yuan, W. Z.; Qin, A.; Lam, J. W. Y.; Sun, J. Z.; Dong, Y.; Haeussler, M.; Liu, J.; Xu, H. P.; Zheng, Q.; Tang, B. Z. *Macromolecules*, **2007, 40**: 3159

14　Percec V.; Asandei, A. D.; Hill, D. H.; Crawford, D. *Macromolecules*, **1999, 32**: 2597

15　Soto, J. P.; Diaz, F. R.; Valle, M. A.; Nunez, C. M.; Bernede, J. C. *Euro. Polym. J.*, **2006, 42**: 935

16　Zhao, X.; Hu, X.; Zheng, P. J.; Gan, L. H.; Lee, C. K. P. *Thin Solid Films*, **2005, 477**: 88

17　Lam, J. W. Y.; Dong, Y.; Kwok, H. S.; Tang, B. Z. *Macromolecules*, **2006, 39**: 6997

18　Suda, K.; Akagi, K. *J. Polym. Sci. A-Polym. Chem.*, **2008, 46**: 3591

19　Goto, H.; Dai, X.; Narihiro, H.; Akagi, K. *Macromolecules*, **2004, 37**: 2353

20　Goto, H.; Dai, X.; Ueoka, T.; Akagi, K. *Macromolecules*, **2004, 37**: 4783

21　O′Neill, M.; Kelly, S. M. *Adv. Mater.*, **2003, 15**: 1135

22　Lam, J. W. Y.; Dong, Y.; Cheuk, K. K. L.; Luo, J.; Xie, Z.; Kwok, H. S.; Mo, Z.; Tang, B. Z. *Macromolecules*, **2002, 35**: 1229

23　Dong, Y.; Lam, J. W. Y.; Han. P.; Cheuk, K. K. L.; Kwok, H. S.; Tang, B. Z. *Macromolecules*, **2004, 37**: 6408

24　Ravichandar, R.; Thelakkat, M.; Somanathan, N. *J. Fluoresc.*, **2008, 18**: 891

25　Kijima, M. Akagi, K.; Shirakawa, H. *Synth. Met.*, **1997, 84**: 313

26　Sohn, H. S.; Yoon, Y. S.; Lee, J. C. Synthsis and characterization of novel polythiophene derivatives: the effect of side chain hydrophilicity on the mesomorphic behaviors of the polythiophene. Abstracts of Papers 236th ACS National Meeting, Philadelphia, PA, United States, August 17-21, 2008: 468

27　Dai, X. M.; Narihiro, H.; Goto, H.; Akagi, K.; Yokoyama, H. *Synth. Met.*, **2001, 119**: 397

28　Jin, S. H.; Lee, H. J.; Sun, Y. K.; Kim, H. D.; Koh, K. N.; Gal, Y. S.; Park, D. K. *Euro. Polym. J.*, **1999, 35**: 89

29　Goto, H.; Akagi, K.; Dai, X.; Narihiro, H. *Ferroelectrics*, **2007, 348**: 149

30　Osaka, I.; Shibata, S.; Toyoshima, R.; Akagi, K.; Shirakawa, H. *Synth. Met.*, **1999, 102**: 1437

31　Dai, X. M.; Goto, H.; Akagi, K.; Shirakawa, H. *Synth. Met.*, **1999, 102**: 1291

32　Toyoshima, R.; Narita, M.; Akagi, K.; Shirakawa, H. *Synth. Met.*, **1995, 69**: 289

33　Hiroyuki, K.; Fumio, S.; Takashi, M.; Naoyuki, K. *Polym. J.*, **2003, 35**: 945

34 Radhakrishnan, S.; Somanathan, N.; Narashimhaswamy, T.; Thelakkat, M.; Schmidt, H. W. *J. Therm. Anal. Calor.*, **2006, 85**: 2433

35 Hird, M.; Toyne, K. J.; Gray, G. W.; Day, S. E.; McDonnell, D. G. *Liq. Cryst.*, **1993, 15**: 122

36 Goulding, M.; Green, S.; Parri, O.; Coates, D. *Mol. Cryst. Liq. Cryst.*, **1995, 265**: 27

37 Zhou, D.; Chen, Y. W.; Chen, L.; Zhou, W. H.; He, X. H. *Macromolecules*, **2009, 42**: 1454

38 Chen, L.; Chen, Y. W.; Zhou, W. H.; He, X. H. *Synth. Met.*, **2009, 159**: 576

39 Chen, L.; Chen, Y. W.; Yao, K.; Zhou, W. H.; Li, F.; Chen, L.; Hu, R.; Tang, B. Z. *Macromolecules*, **2009, 42**: 5053

40 Chen, L.; Chen, Y. W.; Yao, K.; Zhou, W. H.; Li, F.; Chen, L.; Hu, R.; Tang, B. Z. *J. Polym. Sci. A-Polym. Chem.*, **2009, 47**: 4723

41 Chen, L.; Chen, Y. W.; Zhou, W. H.; He, X. H. *Mol. Cryst. Liq. Cryst.*, **2009,** in press

42 Chen, L.; Chen, Y. W.; Zha, D. J.; Yang, Y. *J. Polym. Sci. A-Polym. Chem.*, **2006, 44**: 2499

43 Okano, Y.; Masuda, T.; Higashimura, T. *J. Polym. Sci. Polym. Chem. Ed.*, **1985, 23**: 2527

44 Lam, J. W. Y.; Tang, B. Z. *Acc. Chem. Res.*, **2005, 38**: 745

45 Goto, H. *Macromolecules*, **2007, 40**: 1377